Superconductivity in $A_{1.5}$phenanthrene (A=Sr,Ba)

X. F. Wang,[1] Y. J. Yan,[1] Z. Gui,[2] R. H. Liu,[1] J. J. Ying,[1] X. G. Luo,[1] and X. H. Chen[1,*]

[1]*Hefei National Laboratory for Physical Science at Microscale and Department of Physics, University of Science and Technology of China, Hefei, Anhui 230026, People's Republic of China*

[2]*State Key Laboratory of Fire Science, University of Science and Technology of China, Hefei, Anhui 230026, China*

We discover superconductivity in alkali-earth metal-doped phenanthrene. The superconducting critical temperatures T_c are 5.6 and 5.4 K for Sr$_{1.5}$phenanthrene and Ba$_{1.5}$phenanthrene, respectively. The shielding fraction of Ba$_{1.5}$phenanthrene exceeds 65%. The Raman spectra show 8 and 7 cm^{-1}/electron downshifts for the mode at 1441 cm^{-1} due to the charge transfer to organic molecules from the dopants of Ba and Sr. Similar behavior has been observed in A_3phenanthrene and A_3C$_{60}$ (A = K and Rb). The positive-pressure effect in Sr$_{1.5}$phenanthrene and Ba$_{1.5}$phenanthrene together with the lower T_c with a larger lattice indicates unconventional superconductivity in this organic system.

PACS number(s): 74.70.Kn, 74.62.Fj, 74.25.−q

I. INTRODUCTION

Superconductors, materials that conduct electricity without resistance and completely eject the magnetic-field lines,[1] are mostly inorganic materials.[2–6] Organic superconductors are very intriguing in the condensed-matter physics community due to low dimensionality, strong electron-electron and electron-phonon interactions, and the proximity of antiferromagnetism, insulator states, and superconductivity. Basically, there are mainly two types of organic superconductors: (i) the quasi-one-dimensional Bechgaard and Fabre salts tetramethyltetraselenafulvalene (TMTSF)$_2X$ (Ref. [7]) and tetramethyltetrathiafulvalene (TMTTF)$_2X$ (X = monovalent anions) (Ref. [8]) and (ii) quasi-two-dimensional salts derived from the donor molecule [bis(ethylenedithio)tetrathiafulvalene] (BEDT-TTF)$_2X$ (Ref. [9]). The recent discovery of superconductivity in doped organic crystals containing an extended phenanthrene-like structural motif,[10] which is designated as [n]phenacens [n = 3 (Ref. [11]) and 5 (Ref. [12])], has provided a new empirical substance for the occurrence of superconductivity in organic π-molecular materials. Organic materials generally are considered as electrical insulators. Both phenanthrene (n = 3) and picene (n = 5) are semiconductors with band gaps of 3.16 (Ref. [13]) and 3.3 eV (Ref. [12]), respectively. Superconductivity is introduced by doping alkali metals into the interstitial sites of the pristine compounds. The charge (electron) transfer from alkali-metal atoms to the molecules results in changes in the electronic structure and the physical properties to realize superconductivity.

All the reported organic superconductors, including the doped phenanthrene type, contain five-member rings or six-member rings with conjugated π-orbital interactions among these rings. The π-electron can delocalize throughout the crystal, giving rise to metallic conductivity due to a π-orbital overlap between adjacent molecules. The molecule and crystal structure of organic materials are completely different from the inorganic system, which makes the understanding of superconductivity in organic systems quite difficult and complicated. The superconductivity in doped phenanthrene-type materials offers an excellent candidate for studying physics in organic π-molecular superconductors. However, the superconducting fraction was reported to be rather small in both phenanthrene and picene systems. The maximum shielding fractions in the powder samples of K-doped picene and phenanthrene are 1.2% (Ref. [12]) and 5.3% (Ref. [11]), respectively. This makes it difficult to investigate intrinsic superconducting properties in phenanthrene-type systems. Obtaining high-quality samples and pursuing new superconductors in this hydrocarbon superconducting family are the central issues for investigating intrinsic physical properties and understanding the superconducting mechanism in organic π-molecular superconductors. Here, we report the discovery of superconductivity in strontium- and barium-doped phenanthrene, and the superconducting transition temperature is a T_c of 5.6 and 5.4 K for Sr$_{1.5}$phenanthrene and Ba$_{1.5}$phenanthrene, respectively. The shielding fraction is up to 65.4% in Ba$_{1.5}$phenanthrene at 2 K. Raman spectra show 8 and 7 cm^{-1}/electron downshifts due to the charge transfer, which are similar to those of A_3phenanthrene and A_3C$_{60}$ (A = K and Rb). The pressure dependence of superconductivity shows a positive coefficient $d[T_C/T_C(0)]/dP$ and an enhancement of the shielding fraction.

II. EXPERIMENTAL

Barium (99%), strontium (99%), and phenanthrene (98%) were purchased from Alfa Aesar. The phenanthrene was purified by the sublimation method.[11] Barium and strontium were ground into powder with a file. The purified phenanthrene and Ba/Sr powder were mixed with a chemical stoichiometry ratio. The mixture was ground carefully and then was pressed into pellets. The samples were sealed in a quartz tube under vacuum at less than 5×10^{-4} Pa. The sample was heated to 230 °C for 8 days with intermediate grinding and pelleting three times. Finally, the products with a uniform dark black color were obtained. The x-ray diffraction (XRD) and Raman measurement were carried out by sealing the samples in capillaries, which were made of special glass No. 10 and purchased from Hilgenberg GmbH.

III. RESULTS AND DISCUSSIONS

Figure 1 shows the XRD patterns of the pure and Ba- and Sr-doped phenanthrene, respectively. Figure 1(a) shows the XRD pattern of pure phenanthrene. There are three fused benzene rings in the molecule of phenanthrene as shown
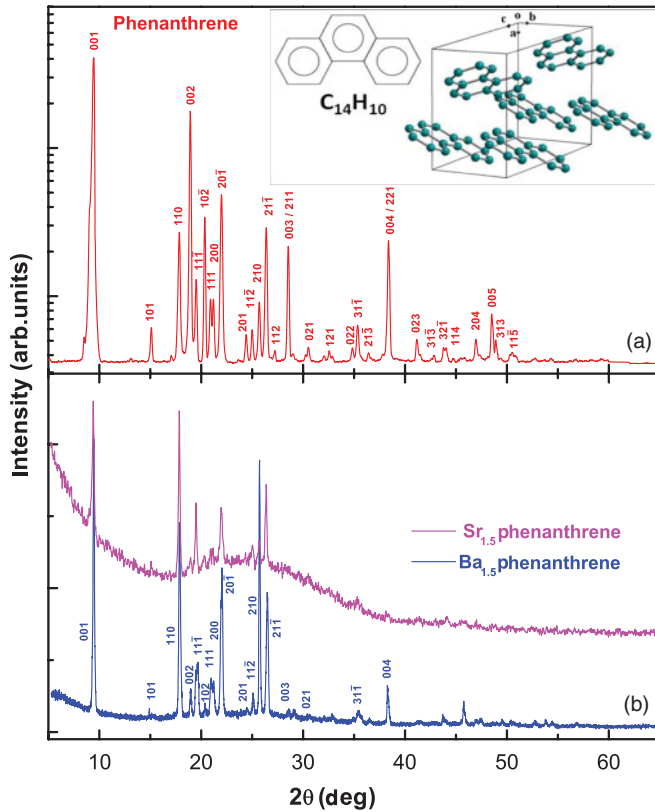
FIG. 1. (Color online) XRD patterns for phenanthrene, $Sr_{1.5}$phenanthrene, and $Ba_{1.5}$phenanthrene. (a) XRD patten for pristine phenanthrene, the molecule and crystal structure are shown in the inset. (b) XRD patterns for Sr- and Ba-doped phenanthrene.

in the inset of Fig. 1(a). The phenanthrene crystallizes in the space group of $P2_1$. The lattice parameters for pristine phenanthrene are $a = 8.453$, $b = 6.175$, $c = 9.477$ Å, and $\beta = 98.28°$, being consistent with the results reported before.[14] Figure 1(b) shows the XRD patterns of Sr- and Ba-doped phenanthrene, respectively. All the peaks can be indexed well with the $P2_1$ space group. No impurity phase was found in the XRD pattern. Lattice parameters are $a = 8.471$, $b = 6.181$, $c = 9.491$ Å, and $\beta = 97.55°$ for $Sr_{1.5}$phenanthrene; $a = 8.479$, $b = 6.177$, $c = 9.502$ Å, and $\beta = 97.49°$ for $Ba_{1.5}$phenanthrene. It indicates that the superconducting phase discussed below is responsible for the superconductivity. The lattice parameters show slight changes compared to pristine phenanthrene. The unit-cell volume increases slightly from 489.5 Å^3 for phenanthrene to 492.6 Å^3 for $Sr_{1.5}$phenanthrene and 493.4 Å^3 for $Ba_{1.5}$phenanthrene, which is consistent with the doped TMTSF case. With a monovalent-anion injection, the unit-cell volume of $(TMTSF)_2PF_6$ expands to 345.5 Å^3 per TMTSF molecule from 316 Å^3 per TMTSF in the pristine compound.[15] Whereas, in K_x picene, the unit-cell volume shows significant shrinkage due to potassium doping.[12] Generally, there are two effects of foreign atom/ionic intercalation on the unit-cell volume. First, the lattice will expand because of the volume of the foreign atom. Second, the attracting force will become an electrostatic attraction from the Van der Waals force, which will reduce the unit-cell volume. The change in lattice parameter induced by the intercalation
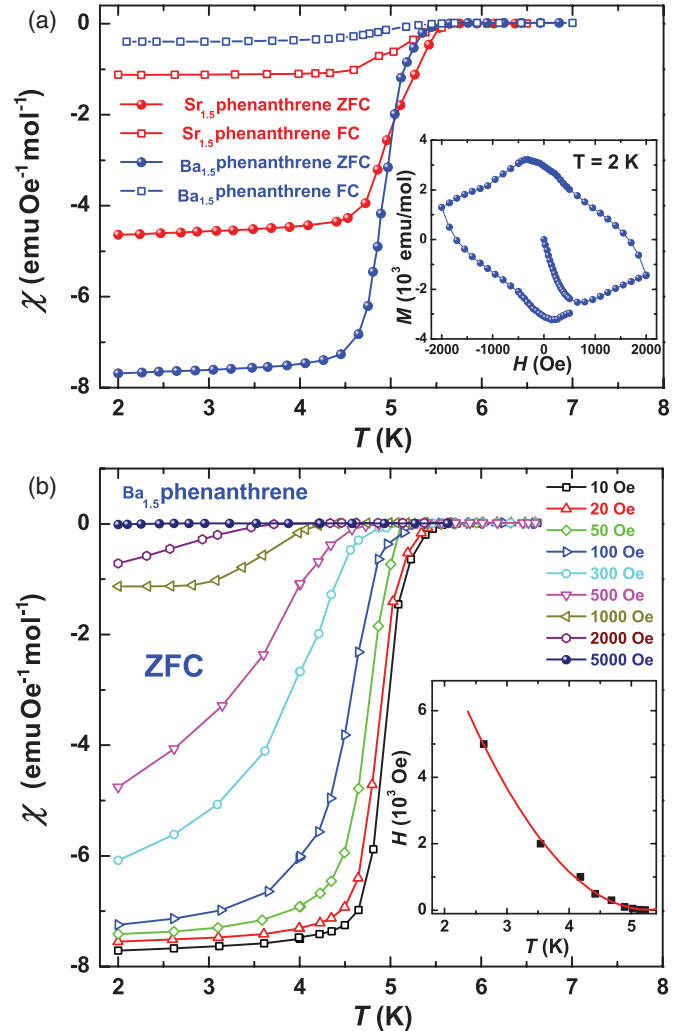
FIG. 2. (Color online) Temperature dependence of magnetic susceptibility (χ) for $Sr_{1.5}$phenanthrene and $Ba_{1.5}$phenanthrene. (a) χ versus T plots for $Sr_{1.5}$phenanthrene and $Ba_{1.5}$phenanthrene in the zero-field-cooling (ZFC) and FC measurements under a magnetic field of 10 Oe. The inset shows the M-H curve of $Ba_{1.5}$phenanthrene at 2 K. (b) χ versus T curve for $Ba_{1.5}$phenanthrene in the ZFC measurements under different magnetic fields. The H versus T_c plot is shown in the inset.

of Sr and Ba indicates the former factor contributes more in Sr- and Ba-doped phenanthrene to affect the crystal structure.

Figure 2(a) shows the temperature dependence of magnetic susceptibility χ for the powder samples of $Sr_{1.5}$phenanthrene and $Ba_{1.5}$phenanthrene in the ZFC and FC processes under a magnetic field of 10 Oe. Susceptibility shows a drastic drop in ZFC and FC measurements at 5.6 and 5.4 K for $Sr_{1.5}$phenanthrene and $Ba_{1.5}$phenanthrene, respectively. The temperature corresponding to the sharp drop is defined as the superconducting transition temperature (T_c). The T_cs for the present two compounds are higher than those of 4.95 and 4.75 K for K_3phenanthrene and Rb_3phenanthrene, respectively. The intercalation of a larger atom results in a lower T_c, which is consistent with the alkali-metal-doped phenanthrene. The evolution of T_c with the radii of intercalating atoms for doped phenanthrene is quite different from the doped
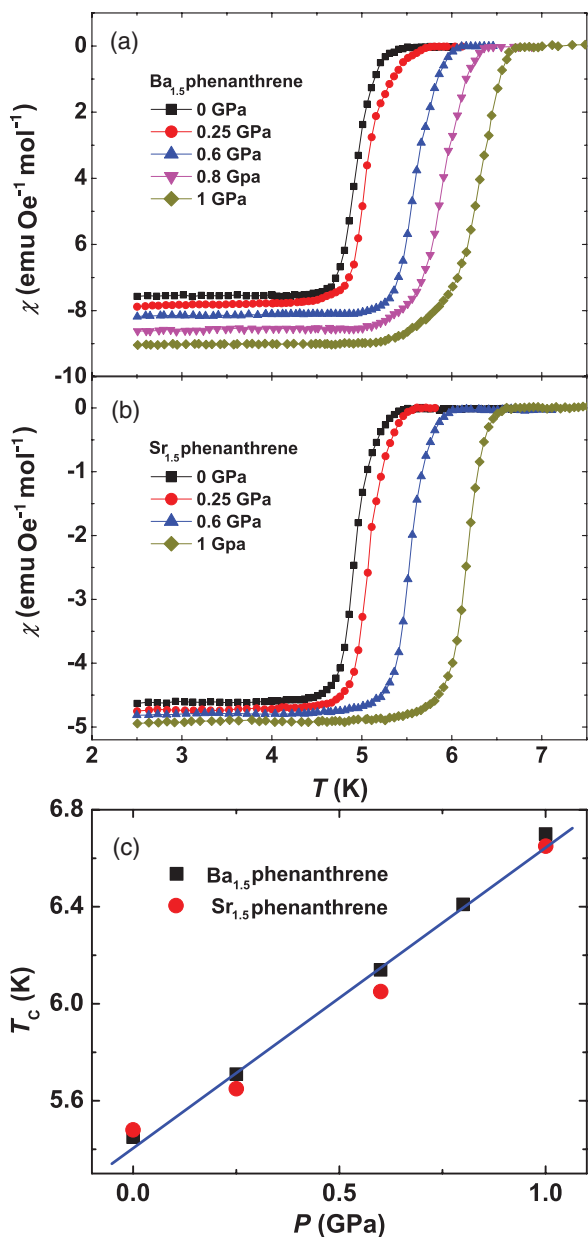
FIG. 3. (Color online) Pressure dependence of superconducting transition temperature T_c for $Sr_{1.5}$phenanthrene and $Ba_{1.5}$phenanthrene. (a) Magnetic susceptibility χ versus T in the ZFC measurements for $Ba_{1.5}$phenanthrene under the pressures of $P = 0$, 0.25, 0.6, 0.8 and 1.0 GPa. (b) Magnetic susceptibility χ versus T in the ZFC measurement for $Sr_{1.5}$phenanthrene under different pressures of $p = 0$, 0.25, 0.6 and 1.0 GPa. (c) Pressure dependence of T_c for superconducting $Ba_{1.5}$phenanthrene and $Sr_{1.5}$phenanthrene.

C_{60}, whose superconducting transition temperatures increase monotonically as the unit-cell size increases.[16] It cannot be understood in BCS theory because the density of states (DOS) increases with lattice expansion, and an increase in the DOS should lead to an enhancement of T_c based on BCS theory. However, the T_c of $Sr_{1.5}$phenanthrene is little higher than that of $Ba_{1.5}$phenanthrene with a larger unit-cell volume. In this sense, $Sr_{1.5}$phenanthrene and $Ba_{1.5}$phenanthrene superconductors should be unconventional. Diamagnetic signals

from ZFC and FC measurements can be assigned to shielding and Meissner effects. As shown in Fig. 2(a), the shielding fraction and the Meissner fraction are 65.4% and 3.4% for the powder sample of $Ba_{1.5}$phenanthrene, 39.5% and 9.5% for the sample of $Sr_{1.5}$phenanthrene, respectively. The shielding fraction is much larger than that of alkali-metal-doped picene and phenanthrene. The superconducting transition width is ~ 0.8 K, which is comparable with K_3phenanthrene and Rb_3phenanthrene. The M versus H plot is shown as the inset of Fig. 2(a). The lower critical field H_{C1} of $Ba_{1.5}$phenanthrene is 720 Oe at 2 K, which is larger than the value of 380 Oe at 5 K in $K_{3.3}$ picene with a T_c of 18 K and 175 Oe at 2 K in K_3phenanthrene with a T_c of 5 K.

Figure 2(b) shows χ versus T plots for the $Ba_{1.5}$phenanthrene superconductor under different magnetic fields. The diamagnetic signal gradually was suppressed, and the superconducting transition became significantly broad with the application of magnetic fields. One clearly can observe a superconducting transition at 3.5 K with a magnetic field up to 2000 Oe. When the field is higher than 5000 Oe, it is difficult to observe the superconducting transition from the magnetization curve. The magnetic-field H versus T_c plot is shown in the inset of Fig. 2(b). It is difficult to precisely determine the upper critical field H_{C2} from the H-T_c curve, but it is obvious that it exceeds 2000 Oe.

Figures 3(a) and 3(b) show the temperature dependence of χ for $Sr_{1.5}$phenanthrene and $Ba_{1.5}$phenanthrene, respectively, in ZFC measurements under different pressures. The most remarkable result is that the T_c for both $Sr_{1.5}$phenanthrene and $Ba_{1.5}$phenanthrene increases with increasing applied pressure. The shielding fraction also becomes larger. It indicates that the superconductivity is enhanced with the pressure. As shown in Fig. 3(c), $d[T_c(P)/T_c(0)]/dP$ are ~ 0.21 and 0.23 GPa^{-1} for $Sr_{1.5}$phenanthrene and $Ba_{1.5}$phenanthrene, respectively. The positive-pressure effect is similar to that of K_3phenanthrene. According to BCS theory, the decrease in T_c is expected with an application of pressure because the application of pressure leads to a contraction of the lattice, and consequently, then the DOS $N(E_F)$ at the Fermi level decreases. The
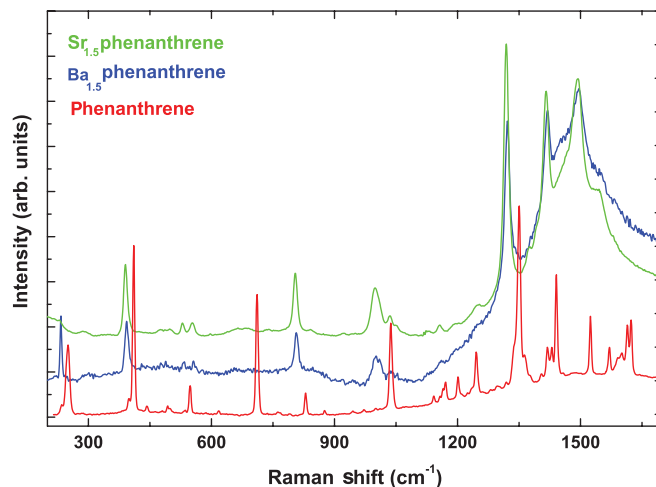
FIG. 4. (Color online) Raman spectra for the pure phenanthrene, the superconducting $Sr_{1.5}$phenanthrene, and the $Ba_{1.5}$phenanthrene.

unusual positive-pressure effect indicates unconventional superconductivity in $Sr_{1.5}$phenanthrene and $Ba_{1.5}$phenanthrene superconductors.

Figure 4 shows the Raman scattering for pristine phenanthrene, $Sr_{1.5}$phenanthrene, and $Ba_{1.5}$phenanthrene. There are seven major peaks in pristine phenanthrene: 1524, 1441, 1350, 1037, 830, 411, and 250 cm^{-1}. The major peaks of the Raman spectrum belong to the A_1 mode due to the C-C stretching vibration.[17,18] The phonon modes in $Sr_{1.5}$phenanthrene and $Ba_{1.5}$phenanthrene show redshifts relative to the pristine phenanthrene. Such a phonon-mode softening effect arises from the charge transfer into the phenanthrene molecule from dopants of Ba and Sr. The main mode shifts from 1441 cm^{-1} in pristine phenanthrene to 1416 cm^{-1} in $Sr_{1.5}$phenanthrene and 1419 cm^{-1} in $Ba_{1.5}$phenanthrene. There are 25 and 22 cm^{-1} downshifts for $Sr_{1.5}$phenanthrene and $Ba_{1.5}$phenanthrene, respectively. It indicates an 8-cm^{-1}/electron downshift for $Sr_{1.5}$phenanthrene and a 7-cm^{-1}/electron downshift for $Ba_{1.5}$phenanthrene due to the charge transfer. This is consistent with that of K_3phenanthrene (6 cm^{-1}/electron) and Rb_3phenanthrene (7 cm^{-1}/electron). Such similar behavior has been observed in A_3C_{60} ($A =$ K,Rb,Cs) in which a 6 cm^{-1}/electron redshift at 1460 cm^{-1} occurs.[19] The Raman shift induced by charge transfer is nearly the same and is independent of dopants, being similar to that of alkali-metal-doped C_{60}.

IV. SUMMARY

To summarize, we discovered the superconductivity in Sr- and Ba-doped phenanthrene-type systems. $Sr_{1.5}$phenanthrene and $Ba_{1.5}$phenanthrene show a superconductivity at 5.6 and 5.4 K, respectively. The positive-pressure effect in $Sr_{1.5}$phenanthrene and $Ba_{1.5}$phenanthrene and a lower T_c with a larger lattice indicate unconventional superconductivity in this organic system. The superconductivity can be realized by doping alkali-earth metals to provide charge and to transfer it to organic molecules.

*chenxh@ustc.edu.cn

[1]*Handbook of Superconductivity*, edited by C. P. Poole Jr. (Academic, San Diego, 2000).

[2]H. K. Onnes, Commun. Phys. Lab. Univ. Leiden **12**, 120 (1911).

[3]G. I. Oya and E. J. Saur, J. Low Temp. Phys. **34**, 569 (1979).

[4]B. T. Matthias, T. H. Geballe, S. Geller, and E. Corenzwit, Phys. Rev. **95**, 1435 (1954).

[5]J. G. Bednorz and K. A. Mueller, Z. Phys. B **64**, 189 (1986).

[6]Y. Kamihara, T. Watanabe, M. Hirano, and H. Hosono, J. Am. Chem. Soc. **130**, 3296 (2008).

[7]D. Jérome, A. Mazaud, M. Ribault, and K. Bechgaard, J. Phys. Lett. (Paris) **41**, 95 (1980).

[8]S. S. P. Parkin, F. Creuzet, M. Ribault, D. Jérome, K. Bechgaard, and J. M. Fabre, Mol. Cryst. Liq. Cryst. **79**, 605 (1982).

[9]A. M. Kini, U. Geiser, H. H. Wang, K. D. Carlson, J. M. Williams, W. K. Kwok, K. G. Vandervoort, J. E. Thompson, and D. L. Stupka, Inorg. Chem. **29**, 2555 (1990).

[10]F. B. Mallory, K. E. Butler, A. C. Evans, E. J. Brondyke, C. W. Mallory, C. Q. Yang, and A. Ellenstein, J. Am. Chem. Soc. **119**, 2119 (1997).

[11]X. F. Wang, R. H. Liu, Z. Gui, Y. L. Xie, Y. J. Yan, J. J. Ying, X. G. Luo, and X. H. Chen, Nat. Commun. **2**, 507 (2011).

[12]R. Mitsuhashi, Y. Suzuki, Y. Yamanari, H. Mitamura, T. Kambe, N. Ikeda, H. Okamoto, A. Fujiwara, M. Yamaji, N. Kawasaki, Y. Maniwa, and Y. Kubozono, Nature (London) **464**, 76 (2010).

[13]M. T. Bhatti, M. Ali, G. N. Shahid, M. Saleh, and A. M. Rana, Turk. J. Phys. **24**, 673 (2000).

[14]J. Trotter, Acta Crystallogr. **16**, 605 (1963).

[15]J. Y. Kim, M. Yun, D. W. Jeong, J. J. Kim, and I. J. Lee, J. Korean Phys. Soc. **55**, 212 (2009).

[16]R. M. Fleming, A. P. Ramirez, M. J. Rosseinsky, D. W. Murphy, R. C. Haddon, S. M. Zahurak, and A. V. Makhija, Nature (London) **352**, 787 (1991).

[17]J. M. L. Martin, J. E. Yazal, and J. P. Francois, J. Phys. Chem. **100**, 15358 (1996).

[18]J. Godec and L. Colombo, J. Chem. Phys. **65**, 4693 (1976).

[19]P. Zhou, K. A. Wang, Y. Wang, P. C. Eklund, M. S. Dresselhaus, G. Dresselhaus, and R. A. Jishi, Phys. Rev. B **46**, 2595 (1992).